

MECHANISMS OPERATING AT A JETTIED RIVER ENTRANCE

Bruce M. Druery
Supervising Engineer,
Estuary Process Investigations

Alexander F. Nielsen
Engineer
Coastal Process Investigations

Department of Public Works, State Office Block,
Phillip Street, Sydney, AUSTRALIA. 2000

ABSTRACT

Between October 1976 and July 1977 a northern rubble mound jetty was constructed at the mouth of the Hastings River, transforming the entrance from a single to a double jettied system. Prior to the jetty construction the entrance was characterised by the presence of a substantial swash bar (alternatively called an ebb delta marginal shoal) which was a continuous feature over 100 years of hydrographic survey records. However, construction of the northern jetty triggered an unprecedented onshore movement of the swash bar. This movement was well documented by a field monitoring programme incorporating hydro-surveys, aerial photographs, tidal gaugings, sediment sampling, float tracking and nearby wave rider buoy information.

A semi-quantitative model was developed to aid understanding and quantification of the macro sedimentary processes associated with this phenomenon. The model demonstrated that the sudden reduction of the swash bar was due to the disruption of a circulation of sand which had previously aided the dynamic stability of the bar. The quantitative predictions of the model agreed well with subsequent entrance behaviour. The philosophical development of the model and its findings are discussed in detail.

In the literature there is a general lack of attempts to quantify the sediment transport relationships between the gross morphologic features of tidal entrances. This paper presents a methodology for assessing the sedimentary process at tidal entrances.

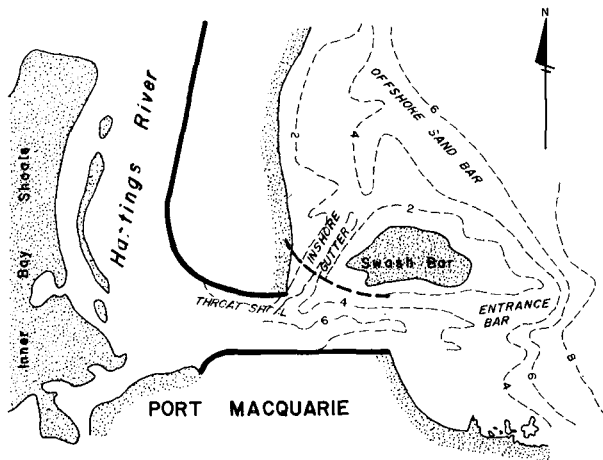
1. INTRODUCTION

The coastline of New South Wales has over thirty jettied river entrances. Their physical setting varies from the sandy (albeit eroding) coastline of the north, characterised by relatively high littoral drift rates, to the southern coastline where pocket beaches and prominent rocky headlands extending into deep water testify to an impoverished littoral drift. Virtually all these entrances have river mouth bars and entrance jetties have been constructed to satisfy, to varying degrees, the navigational requirements of increased depth, safer navigation and/or stability of inlet location. This paper is a critical review of the response of the Hastings River, Port Macquarie, to recent entrance jetty construction.

Port Macquarie is located at the mouth of the Hastings River, in the mid-north coast of N.S.W. - See fig. 1. Tides are semi-diurnal



PORT MACQUARIE DEFINITION SKETCH



- KEY**
- Low water (L.W.O.S.T.)
 - Early training works - Southern 1897
- Northern 1940
 - - - New entrance jetty 1977 / '78
 - - - Contours - metres, 1966 survey
- metres 0 200 400

Figures 1 and 2

with a Mean Spring Tide range, at the entrance, of 1.26 m associated with a peak tidal discharge of 1600 cumecs. Fluvial flows are flashy but significant. The peak fluvial discharge is 7100 cumecs, estimated from height records spanning the last 50 years. The wave climate is moderate to high with offshore significant wave heights of 1.5 m being exceeded 50% of the time (Lawson and Abernathy 1975).

Since its discovery in 1819 by Captain John Oxley the Hastings River entrance has been hazardous

to navigate. Records are replete with accounts of vessels running aground on the bar or being swamped and even wrecked. Navigation of any entrance bar is never easy and the Hastings River bar can be treacherous because it is unusually wide, has a steep seaward face and a shifting channel.

2. HISTORY OF ENTRANCE WORKS AT PORT MACQUARIE

The first attempts to stabilise the entrance were made in 1897 when construction was started on the southern training wall and jetty - see fig. 2. These works proved to be largely ineffectual with the entrance varying in position over a distance of 1 km along the northern beach. The pattern was for floods to cut through the northern sandspit and the new entrance to migrate slowly southwards.

A northern training wall and jetty were completed in 1940 but the works were gradually out flanked by the prograding profiles of the adjacent beaches.

During the last decade the entrance has been host to a broad expanse of shoals through which the channel has shifted seasonally according to the prevailing wave pattern. The deterioration of the bar has had a deleterious effect on the local fishing and commercial fishing industries and prevented Port Macquarie from realising its full tourist and pleasure craft potential (Posford, et al 1974). Hence in October 1976 construction of a new northern jetty commenced with the objective of creating a more stable, safer bar for navigation.

Since the commencement of construction a field monitoring programme has been in operation and considerable data relating to the morphologic changes in the entrance area has been obtained.

3. SEDIMENTARY PROCESSES

To facilitate discussion of sedimentary processes the study area has been subdivided into a number of coastal cells - see fig. 3. The cells have been chosen because they comprise a number of discrete hydraulic processes and it is useful to discuss the interactions of these processes within relatively self-contained cells. Interactions between cells link them together as a complete dynamic system. The detailed discussion of data and the quantification of the processes is given by Druery and Nielsen (1979) and only the key findings will be discussed below.

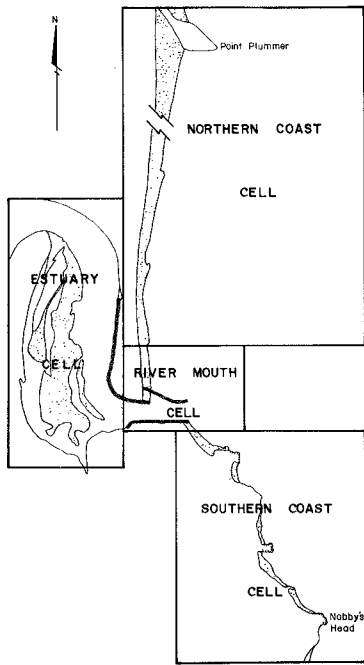


Figure 3 Coastal Cells

3.1 Estuary Cell

This cell is defined as that part of the river upstream of the entrance throat and includes the inner bay shoals. An analysis of 14 hydrographic surveys, from 1881 to 1972, demonstrated that the inner shoals showed an early tendency towards accretion due to the high sand infill rates prior to the construction of the northern training wall in 1940. Since that time the inner shoals have tended to stabilise

and the contemporary growth rate was estimated at $50,000 \text{ m}^3$ per year.

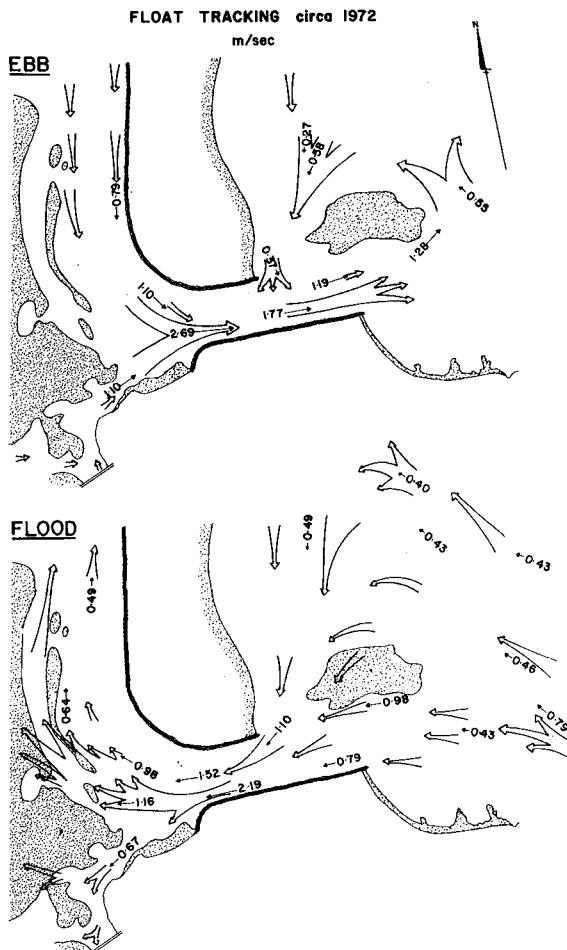


Figure 4 shows the results of float tracking carried out in 1972. The flood tides promote accretion of the inner bay shoals due to the direct impingement of the flood tide velocities. The ebb velocities are basically parallel to the training wall and hence tend to interact little with the bulk of the inner shoals. This tendency for net flood tide accretion manifests itself as a growth of parallel, crescentic shaped shoals on the eastern edge of the inner shoals - see fig. 5. There appears to be a functional relationship between accretion and the throat shoal as seen by the close association of the more recent

Figure 4 Float Tracking Results

crescent (fig. 5) with sand coming from the throat shoal.

Tidal velocities and surface gradients, over a full ebb and flood tide cycle, were measured approx. 1 km upstream from the seaward tip of the southern jetty under conditions of Spring, Neap and intermediate tides. Using these measurements in the sediment transport formula of Ackers and White (1973), the annual transport of sediment by tidal action was estimated to be approximately 200,000 m³ p.a. for the flood tide and 150,000 m³ p.a. for the ebb. Similar sediment transport calculations in the entrance throat indicated a maximum tidal transport capacity of 500,000 m³ p.a. However analysis of bed sediments indicated that the sediments in the entrance throat were coarse and probably predisposed towards armouring. It was considered that because of the high likelihood of channel armouring, the annual transport in the throat would not differ greatly from that estimated for the upstream location. (i.e. there would be 100% throughput of sediment supplied to the throat).

Apart from the tidally active eastern edge of the inner shoals, the bulk of the shoals are relatively stable. Further inland on the shoals diver observations revealed active bioturbation and a surface growth of algae both of which are indicative of immobile sediments. The only note of instability associated with the inner shoals is scouring by floods which tend to remove portions of the crescentic shoals on the eastern margin.

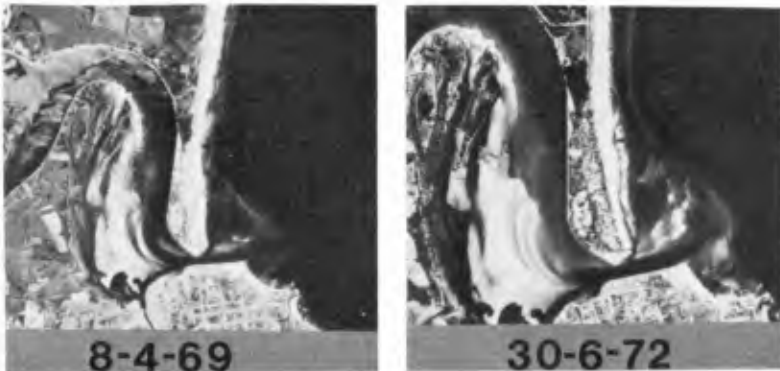


Figure 5 Aerial Photographs showing growth of Inner Shoals.

3.2 River Mouth Cell

The dominant morphologic features of this cell (re: fig. 2) are the entrance bar, the offshore bar, the swash bar, the inshore gutter which separates the swash bar from the beach and the jettied entrance channel and throat shoal.

Current trackings carried out in 1972 (see fig. 4) are typical of the general current patterns which existed prior to the northern jetty construction. While the current trends would depend largely on the conditions pertaining to the particular day of measurement, discussion with the local navigation authority confirmed that fig. 4 is a fair representation of the persistent current features.

A significant feature of the ebb current pattern is the development of a large eddy centred about the swash bar. This is a common feature of tidal inlets, particularly when there is only one entrance jetty (Komar and Terich 1976, FitzGerald et al 1976, Dean and Walton 1975). At Port Macquarie it is considered that the eddy was produced by a combination of factors viz:

1. Viscous drag between the ebb tide jet stream and adjacent water (Dean and Walton 1975).
2. A strong current driving mechanism in the inshore gutter would have been created by the coupling of set down against the northern wall, due to superlevation of the main ebb flow as it was forced around the severe approach bend, and set up due to breaking waves on the swash bar.
3. Refraction of the dominant southeast waves around the swash bar would tend to produce an inlet directed longshore current (Hubbard 1976, Dean and Walton 1975).

During the flood tide the currents seawards of the entrance were generally 50% less.

Irrespective of the state of the tide the currents in the inshore gutter were inlet directed and showed a tendency to increase when the main entrance flow was ebbing. The commitment of the inshore gutter to flood tide currents produced a strong bias in favour of flood tide velocities and sediment transport against the northern training wall.

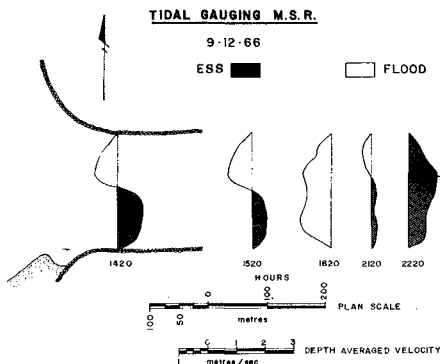
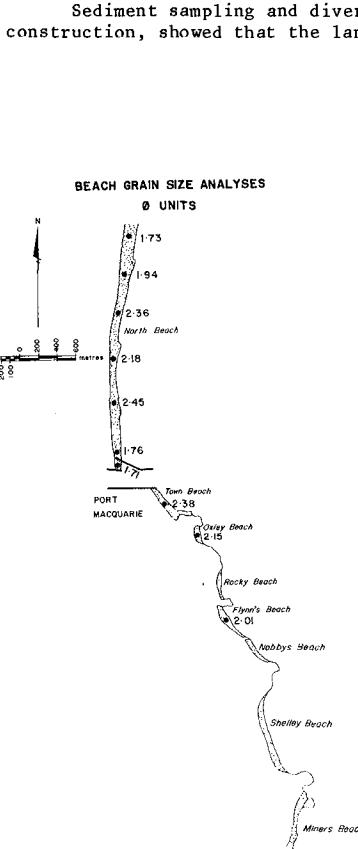


Figure 6 Horizontal Velocity Distribution at Entrance.

Fig. 6 shows portion of comprehensive tidal gaugings carried out in December 1966. Towards the end of the ebb tide the flood tide commenced two hours early against the northern training wall. During the commencement of the ebb tide it persisted for approx. one hour. Hence against the northern wall the flood flow had a duration of 8 hours thus indicating a strong potential for flood tide transport against the northern wall.



Sediment sampling and diver observation, during jetty construction, showed that the landward face of the bar was gravelly comprising well rounded and highly polished shell fragments and lithic pebbles. The surface was formed into symmetrical long crested ripples 7-10 cm in height and 0.3 - 0.6 m wavelength. There was no observed movement of the gravel during conditions of small swell. The seaward face of the bar, however, was composed of shell free quartzose sand and substantial movement of the sand took place (as sheet flow) in response to the orbital velocities of small swell.

The intrinsic difference between the surficial sediments of the inner and outer faces of the bar is intriguing. It is considered that it reflects possible differences in the ebb and flood sediment paths. The ebb tide would tend to jet most of its sediment onto the seaward face of the entrance bar, developing an armouring of the bed of the main channel in the process. During flood tides, the return of that sediment would take place by combined wave and current action on the swash bar and inshore gutter.

On a day to day basis the entrance bar and swash bar constitute a balance between the seaward movement of sediment by the ebb tide and landward transport by waves and the flood tide. The ebb tide would deposit sand on both the entrance bar and the swash bar. Shoaling of waves would induce sediment movement across the surface of the swash bar either onto North Beach or directly onshore and into the inshore gutter.

Figure 7

The inshore gutter would then feed sediment directly into the estuary at all states of the tide and during each ebb tide a significant portion of the inshore gutter sand feed would be carried back onto the swash bar and recycled.

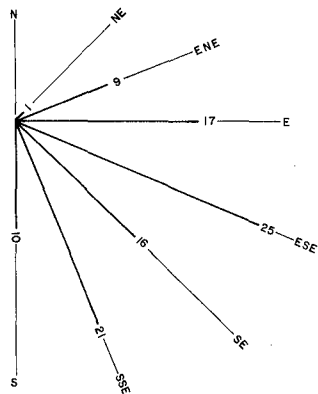
3.3 Southern Coast Cell

This cell comprises small beaches which contain limited sand and are well pocketed between rocky cliffs - see fig. 7. Sedimentological studies identified a distinct northward fining of the beach sands and an absence of lithic minerals, setting them apart from the beach sands of the northern coast cell. All indications pointed to the existence of a weak, intermittent littoral transport which is probably associated with temporary development of offshore bars during major storms and is considered to be of the order of $20,000 \text{ m}^3 \text{ p.a.}$

3.4 Northern Coast Cell

North Beach is zeta shaped with a well developed offshore bar. Historical hydrosurveys revealed episodes of successive onshore and offshore movement of sediments. The offshore sediment movement, resulting from storm events, was of the order of $100-200 \text{ m}^3/\text{m}$ storm whereas onshore movement rates, during calmer periods, were much less and of the order of $30 \text{ m}^3/\text{m/year.}$

PERCENTAGE OCCURRENCE OF WAVE DIRECTION



DATA SOURCE: Wave Rider Buoy;
Coffs Harbour Jun.'75-Nov.'79

Wave refraction analyses were carried out with the aim of assessing longshore sediment transport rates at a number of locations on the beach. The direction of wave approach was divided into two directions; north easterly and south easterly. The percentage occurrence of waves from each direction was set at 19% and 81% respectively, based on four years of wave rider buoy data at Coffs Harbour - see fig. 8. For each direction, four classes of wave height were considered and a representative significant wave height was assigned to each class. From relationships of significant wave height and period derived from the wave rider buoy data a significant wave period was assigned to each representative significant wave height. These parameters are set out in Table 1.

Figure 8

TABLE 1. Representative Wave Statistics used in Refraction Analysis

Significant Wave Height Class	Hs (m)	Representative Wave Height Hs (m)	Wave Period Ts (s)
0 - 1		0.5	6.4
1 - 2		1.5	7.7
2 - 5		3.5	8.9
> 5		7.5	10.2

The occurrence of each representative wave height was determined from wave height exceedance curves presented by Lawson and Abernathy (1975).

The inshore wave breaking height obtained from the wave refraction analyses, the angle of shore break from aerial photographs and the values of % exceedance were used to estimate the littoral sediment transport. The CERC formula exhibited extreme sensitivity to the wave direction data but the overall result was one of zero net longshore drift on North Beach. However, historical aerial photographs showed that an occasional offshore bar forms around the northern headland of the beach (Point Plummer). This suggests that there is an intermittent northward leakage of sand from the compartment which is consistent with the zeta shape of the beach and the existence of rudimentary transgressive dunes in the far north of the beach. Hence it is considered that there is a weak net northerly longshore drift along North Beach.

Gross sediment transport rates calculated at a point on the northeastern edge of the swash bar indicated a strong net onshore transport, the amount of movement being on order of magnitude higher than that estimated for North Beach.

The gross sediment transport rates calculated using the CERC formula were unrealistically high. Gordon et al (1978) also found this to be the case in studies of other beaches along the New South Wales coastline. Hence, it was not considered valid to directly apply the CERC formula which has been empirically developed from measurements on USA beaches. Nevertheless, it was considered that the CERC formula would provide a reasonable indication of the relative magnitude of transport rates calculated at various locations within a littoral system. Hence the net sediment transport rates along North Beach and the northeastern edge of the swash bar were assigned values of "x" and "10x" respectively. The absolute values of the rates were then determined implicitly using the interaction equations of the sediment budget model (Section 7).

4. LONG TERM SEDIMENT DYNAMICS

On a day to day basis the entrance bar/swash bar appears to constitute a relatively stable dynamic system. However long term

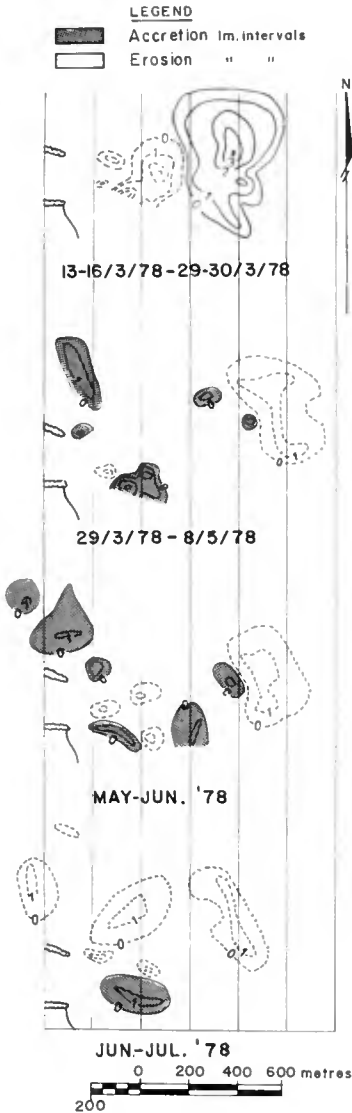


Figure 9 Offshore Isopachs

data (hydrographic surveys and aerial photographs) indicated a cyclicality which can be attributed to the interplay of floods and waves.

Floyd and Druery (1976) found that the seaward face of an entrance bar undergoes movement largely as a result of deposition by floods. Floods deposit sediment on the seaward face in depths of 10 m and less. Hydrographic surveys of the Hastings River bar indicate that the volumes of deposition range from 400,000 m³ to 200,000 m³ for major and moderate floods respectively. Deposition by floods is sudden (i.e. 2 to 3 days). Initially the conditions for navigation on the bar would be good because major floods tend to gouge a gutter through the crest of the bar. This reduces the effective width of the bar and increases the ruling depth, making navigation less hazardous. However Floyd and Druery (1976) showed that any flood deposit, on the seaward face of the bar, would undergo reworking by waves and the pre-flood location of the seaward bar face would tend to be re-established. The onshore movement would be slow and therefore the improved bar conditions would persist for a time varying from six months to two years depending upon the magnitude of the flood. As the relatively slow onshore movement began to have effect, the bar channel would become infilled and conditions on the bar would noticeably deteriorate. The onshore movement would continue until the swash bar invaded the entrance channel. A new flood would restart the cycle.

On 20-23 March 1978 a flood occurred on the Hastings River. Figure 9 shows isopachs of hydrosurveys carried out before and after the flood. It can be seen that the flood deposited sediment on the seaward face of the bar (in depths less than 10 m). The total



Figure 10 16th June '77

Figure 11 15th July '7



Figure 12 26th August '77



Figure 13. 19th December '77

17th July '78
Considerable shore movement
still occurring



21st February '80
Notice shoal area immediately
offshore North Beach

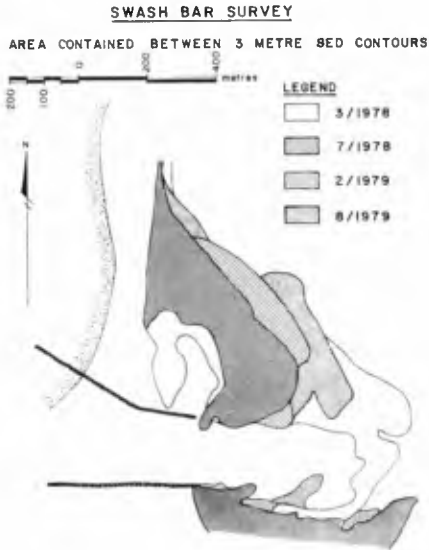


Figure 14

of the sand moving onshore from the swash bar had become attached to the jetty and North Beach as a fillet and the inshore gutter was becoming severely pinched between the tip of the jetty and the advancing slug of sand. The advancing slug of sand had shoaled and its surface was exposed at low water. By August (fig. 12) the slug of sand had completely inundated the inshore gutter and attached itself to North Beach. A portion had been intercepted by the end of the jetty causing the wave trap to be overwhelmed with sand. Spillage of sand from the wave trap had given birth to a fledgling throat shoal. By December (figure 13) the fillet of sand against the base of the jetty had been redistributed along North Beach in the form of a series of wave berms.

The onshore movement of sediment continued well after the completion of construction (viz. July 78) as shown by offshore surveys in figure 14. Between March 78 and August 79 the swash bar progressively reduced in size as a result of this onshore movement.

6. CONCEPTUAL MODEL OF SEDIMENTARY PROCESSES

The investigation of coastal processes in each cell led to the formulation of a conceptual model of the sedimentary processes of the

volume deposited was 280,000 m³ of which 60,000 m³ was derived from scouring of the inner face of the bar. The sequence of post flood surveys shows the seaward face of the bar undergoing reworking and moving slowly onshore as a series of sand slugs.

5. EFFECT OF NORTHERN JETTY

The construction of the northern jetty triggered rapid changes in the estuary mouth morphology - see Figures 10 - 13.

The jetty began to intrude into the surf zone in May 1977 at which time the swash bar occupied a substantial area and the throat shoal had been removed by a small fresh in early May. A month later further extension of the jetty had taken place and a portion of the swash bar had begun to move onshore. See fig. 10. During July (figure 11) some

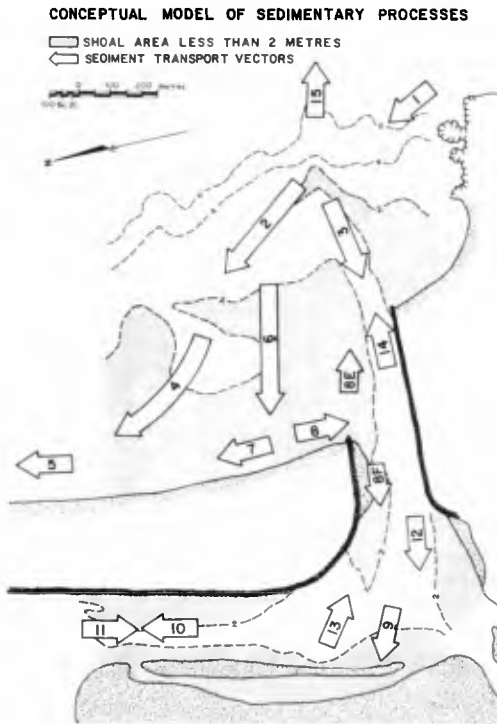
entrance bar and its environs - see Figure 15. In order to test the coherence of the conceptualisation an attempt was made to quantify the various model elements.

6.1 Interaction Equations

Consideration of local sediment budget led to the following interaction equations:

- (1) Sediment moving onshore across the swash bar, Q(2), can either head towards the inshore gutter, Q(6), or travel along the offshore bar (i.e. the outer edge of the swash bar) to North Beach, Q(4).

Hence: $Q(2) = Q(4) + Q(6)$



- (2) Sediment is carried into the estuary, Q(12), by flood currents moving across the entrance bar, Q(3), and via the swash bar/inshore gutter complex, Q(8F).

Hence: $Q(8F) + Q(3) = Q(12)$

- (3) The quantity of sediment dumped on the entrance bar and swash bar each ebb tide, Q(14), is derived from the estuary, Q(11), and the recycled component of the inshore gutter sand feed, Q(8E).

Hence: $Q(14) = Q(8E) + Q(11)$

- (4) Within the estuary the flood tide, Q(12), produces some accretion of the eastern edge of the inner shoals, Q(9), and the rest remains in the active tidal sediment flux, Q(10).

Hence: $Q(12) = Q(9) + Q(10)$

Figure 15 Conceptual Model

- (5) The sediment moving directly onshore from the Swash Bar, $Q(6)$ can split into longshore components $Q(7)$ or $Q(8)$ and $Q(8)$ can be broken down into its ebb and flood constituents.

$$\text{Hence : } Q(6) = Q(7) + Q(8); Q(8) = Q(8E) + Q(8F)$$

- (6) Prior to jetty construction North Beach was relatively stable i.e. $Q(5) = Q(4) + Q(7)$.

6.2 Functional Relationships

- (1) It was assumed that 90% of the flood tide sediment transport took place via the swash bar and inshore gutter i.e. $Q(3) = 0.1 Q(8F)$.

- (2) The ebb and flood sediment transport potential against the inside of the northern training wall was calculated from tidal current measurements assuming transport potential was proportional to the cube of the velocity (Maddock 1969). This indicated that the recycled ebb tide constituent of the inshore gutter sand feed was approximately half the flood tide constituent, therefore

$$Q(8E) = 0.3 Q(8)$$

- (3) The application of the CERC formula to determine the net littoral transport along North Beach, $Q(5)$, and the onshore transport on the Swash Bar, $Q(2)$, was discussed in Section 3.4 where it was argued:

$$Q(2) = 10 Q(5)$$

6.3 Calculated Values

A number of the model elements were known or estimated viz:

- (1) $Q(1) = 20,000 \text{ m}^3 \text{ p.a.}$ (See section 3.3)
- (2) Because currents in the inshore gutter were always inlet directed (Section 3.2) it was assumed that all sand feed would be inlet directed i.e. $Q(7) = 0$
- (3) $Q(9) = 50,000 \text{ m}^3 \text{ p.a.}$ (Section 3.1)
- (4) $Q(12) = 200,000 \text{ m}^3 \text{ p.a.}$ (Section 3.1)
- (5) $Q(11) = 150,000 \text{ m}^3 \text{ p.a.}$ (Section 3.1)
- (6) $Q(13) = \text{Erosion during flood event only}$ (Section 3.1)
- (7) $Q(15) = \text{Deposition during flood events}$ (Section 4)

6.4 Effect of Northern Jetty Construction

The foregoing equations and relationships were adjusted so as to

represent the hydraulic impact of the northern jetty. The impact was divided into the "short term" (i.e. within the first 2-5 years say) and the "long term" (i.e. 10 years or more).

Short Term :

- (1) Because of the elimination of the inshore gutter the majority of sediment moving directly onshore from the swash bar, Q(6), would not find its way into the estuary.

$$\text{i.e. } Q(8) = Q(8F) = Q(8E) = 0$$

- (2) The jetty construction would greatly increase the flood tide velocities across the entrance bar and the tip of the northern jetty and hence the sediment transport capacity of Q(3) would greatly increase. It was considered that the net result would be a reduction in the infeed of sediment into the estuary and hence Q(12) was reduced from its pre-jetty value of 200,000 m³ p.a. to 150,000 m³ p.a.

$$\text{i.e. } Q(12) = 150,000 \text{ m}^3 \text{ p.a.}$$

- (3) It was assumed that initially accretion of the inner shoals would not change i.e. Q(9) = 50,000 m³ p.a.

Long Term :

- (1) After a long period of onshore movement the swash bar would tend to disappear and only an ebb delta bar would remain, similar in shape to other entrances in N.S.W. (Floyd 1968). The only throughput of sediment would be that necessary to bypass the net southerly drift.

$$\text{i.e. } Q(2) = Q(1) = 20,000 \text{ m}^3 \text{ p.a.}$$

- (2) Based on experience of the effects of entrance works at the mouths of other similar estuaries in N.S.W., it was considered that tidal propagation in the estuary would not change significantly and therefore the unusual estuary instability associated with entrance jetty construction at Forster (Gordon and Neilsen, 1980) would not occur.

It was considered that within the estuary a balance would be established but the general level of sediment movement would be less i.e.:

$$Q(10) = Q(11) = 100,000 \text{ m}^3 \text{ p.a.}$$

$$Q(9) = 0$$

Effects of Floods:

It needs to be stressed that the "long term" was considered within the context of no flooding. Floods will tend to place new deposits on the entrance bar (Section 4) which would have the effect of reversing the situation towards the immediate post construction condition.

7. RESULT OF CONCEPTUAL MODEL

All the various functional relationships and known values were applied to the interaction equations for each of the three cases i.e.

- (1) prior to construction
- (2) after construction in the short term
- (3) after construction in the long term

The results are shown in Table 2.

TABLE 2 - Quantification of Conceptual Model

Model Element	Prior to Jetty Const.	After Jetty Short Term	After Jetty Long Term
Q(1)	20,000	20,000	20,000
Q(2)	290,000	290,000	20,000
Q(3)	18,000	150,000	100,000
Q(4)	29,000	29,000	20,000
Q(5)	29,000	29,000	29,000
Q(6)	260,000	260,000	N.A.
Q(7)	0	260,000	N.A.
Q(8)	260,000	0	N.A.
Q(8E)	78,000	0	N.A.
Q(8F)	182,000	0	N.A.
Q(9)	50,000	50,000	0
Q(10)	150,000	150,000	100,000
Q(11)	150,000	100,000	100,000
Q(12)	200,000	150,000	100,000
Q(13)		EXTREME EVENT	
Q(14)	228,000	150,000	100,000
Q(15)		EXTREME EVENT	
Swash Bar Removal Rate i.e. Q(2) + Q(3) - Q(14) - Q(1)	60,000	270,000	N.A.
Sediment Feed to North Beach Q(4) + Q(7)	29,000	289,000	20,000

The main effect of the jetty construction was the elimination of the inshore gutter which used to drive a circulation of sand and therefore tended to perpetuate the swash bar. The recycled component of the inshore gutter sediment feed (i.e. Q(8E)) was of the order of 100,000 m³ p.a.

After jetty construction the swash bar removal rate increased dramatically. This would explain the unprecedented onshore movements observed during the jetty construction (Section 5).

The elimination of the inshore gutter greatly increased the quantities of sediment reaching North Beach and North Beach would therefore be expected to accrete markedly.

The model predicted long term erosion of North Beach viz.:

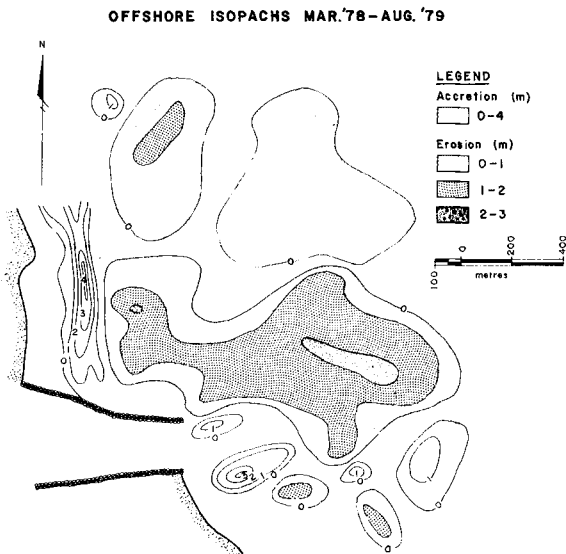
$$Q(5) - Q(4) = 9,000 \text{ m}^3 \text{ p.a.}$$

However, this would tend to be offset (to an unknown extent) by sediment injected into the system by fluvial floods i.e. $Q(15)$.

8. MODEL VERIFICATION

The conceptual model and its predictions were completed by the end of the jetty construction in July 1978. Hence the predictions of the model can be tested against the results of subsequent entrance monitoring.

The progressive decrease in areal extent of the swash bar has already been demonstrated in Figure 14. An Isopach plot between the March and August surveys is shown in figure 16. The broad area of erosion from the swash bar is directly related to pronounced accretionary structures on North Beach (viz. recent beach ridges). Volume calculations indicate a net erosion from the swash bar at a rate of $280,000 \text{ m}^3 \text{ p.a.}$ which compares remarkably well with the estimate of $270,000 \text{ m}^3 \text{ p.a.}$ obtained from the conceptual model.



The pronounced build up of North Beach is compatible with the predicted increase in the sediment supply to North Beach. Estimates of beach accretion were not possible because sediment was dispersed northwards beyond the control area of the beach surveys.

Recent monitoring of the entrance has indicated that the entrance bar has reduced in width and there has been an improvement in bar depth.

Figure 16 Swash Bar and Beach Isopachs

9. CONCLUSIONS

1. For over 40 years the entrance to the Hastings River was host to a large swash bar the presence of which created hazardous navigation conditions. The recent construction of a northern entrance jetty in, 1977-78, triggered an unprecedented onshore movement of the swash bar. The cause can be related to the elimination of a daily circulation of sand which had previously aided the dynamic stability of the swash bar.
2. Monitoring of post-construction changes has indicated that the swash bar will not return to its former size and there has been a substantial reduction in the width of the bar.
3. The long term configuration of the entrance bar and swash bar is linked to the occurrence of major floods. It was possible to discern past cycles of deposition by floods and subsequent slow onshore movement of the flood deposits.
4. It was possible to construct a conceptual model of entrance sedimentary processes which was suitable for predictions of morphological response. Although the model was based on elementary considerations of sediment budget, it was a highly effective tool for elucidating the subtleties of sediment transport relationships between the gross morphologic features of a tidal entrance.

Considerable fundamental research is necessary before full process understanding of tidal entrances will be achieved. Conceptual models as put forward in this paper are a useful interim step which combine the art and the science of coastal engineering and offer a means for assessing the impact of coastal works on macro coastal processes.

10. ACKNOWLEDGEMENTS

The authors acknowledge the assistance of Graeme Levien and Stuart Green in the computation and collation of field data.

11. REFERENCES

- Ackers & White (1973) - Sediment Transport : New Approach and Analysis. Jnl Hyd. Div. ASCE HY11.
- Dean and Walton (1975) - Sediment Transport Processes in the Vicinity of Inlets with Special Reference to Sand Trapping. Est. Res. Vol. 11, Acad. Press.
- Druery & Nielsen (1978) - Port Macquarie Entrance Study. Department of Public Works, N.S.W., Report PWD 78005.

11. REFERENCES (Cont'd).

- Fitzgerald, Nummedal & Kana (1976) - Sand Circulation Pattern at Price Inlet, South Carolina. Proc 15th Int. Conf. Coast. Eng., Hawaii 1976.
- Floyd & Druery (1976) - The Results of River Mouth Training on the Clarence River Bar, N.S.W. Aust., Proc. 15th Int. Conf. Coast. Eng., Hawaii.
- Floyd (1968) - River Mouth Training in New South Wales Proc. Int. Cont. Coast. Eng., 1968.
- Gordon, Lord, Nolan (1978) - Byron Bay - Hastings Point Erosion Study, Department of Public Works, N.S.W., Report No. 78026.
- Komar & Terich (1976) - Changes due to Jetties at Tillamook Bay, Oregon. Proc. 15th Int. Conf. Coast. Eng., Hawaii.
- Lawson & Abernathy (1975) - Long Term Wave Statistics of Botany Bay. 2nd Aust. Conf. Coast & Ocn. Eng., Gold Coast, Queensland.
- Maddock (1969) - The Behaviour of Straight Open Channels with Moveable Beds U.S. Geol. Survey, Prof. Paper 622-A, 70P.
- Nielsen & Gordon (1980) - Tidal Inlet Behavioural Analysis. Proc. 17th Int. Conf. Coast. Eng., Sydney, 1980.
- Posford, Pavry, Sinclair & Knight (1974) - Port Macquarie Economic Study. Report for Department of Public Works.

STABILITY OF ESTUARY MOUTHS IN THE RHINE-MEUSE DELTA

J. VAN DE KREEKE, Professor of Ocean Engineering, Rosenstiel School of Marine and Atmospheric Science, University of Miami, Miami, U.S.A.

JAC HARING, Research Engineer, Deltadienst, Rykswaterstaat, The Hague, Holland

1 GENERAL CHARACTERISTICS OF THE RHINE-MEUSE DELTA

The Rhine-Meuse Delta in the southwestern part of the Netherlands covers an area of approximately 60 x 60 km; see Fig. 1. The Delta consists of sediment deposits of the Rhine and the Meuse in which tides and river flow have scoured an intricate system of channels. The four major estuaries are from south to north Eastern Scheldt, Brouwershavense Gat, Haringvliet and Rotterdam Waterway. The connection between estuaries and rivers is formed by a system of branching channels, referred to as tidal rivers. The flow in the tidal rivers is constrained by dikes, revetments and groynes. It is in this region where most of the sand fraction of the sediments carried by the rivers Rhine and Meuse is deposited. Extensive maintenance dredging is required to maintain a sufficiently large cross-section for navigation. The mud fraction (all sediments with grain size $< 62 \mu$) of the river sediments is carried further seaward and is partly deposited in the estuaries and partly in the offshore underwater delta.

Average tidal ranges at the seaward boundary of the Delta decrease going from south to north and vary between 3.78 m at Flushing to 1.58 m at Hook of Holland. The ratio average tidal range to average spring tidal range is approximately 0.86. Tides are predominantly semi-diurnal. The average annual discharges of the Rhine and Meuse are respectively 2200 m³/sec and 250 m³/sec. Discharges of both rivers show seasonal fluctuations with a maximum in the winter and a minimum at the end of the summer. The river water is distributed over the estuaries in varying proportions. E.g. in 1959 the ratios of the average river volume to the average flood volume for the estuaries Eastern Scheldt, Brouwershavense Gat, Haringvliet and Rotterdam Waterway were respectively 0, 0, 0.25 and 0.53.

In the offshore region there exists a longshore sand motion to the north with a transport rate on the order of 50,000 m³/year. Associated with the longshore motion is a fining of the bottom sand when going from south to north. Typical values for the mean grain diameter of the sand are 200 μ for the mouth of the Eastern Scheldt and 150 μ for the mouth of the Haringvliet. Terwindt (1973).

The present shape of the Delta is to a large extent the result of man's interference with the natural sedimentation processes, the expansion of the port of Rotterdam, maintenance dredging and in particular the Delta project. The Delta project envisions the closure

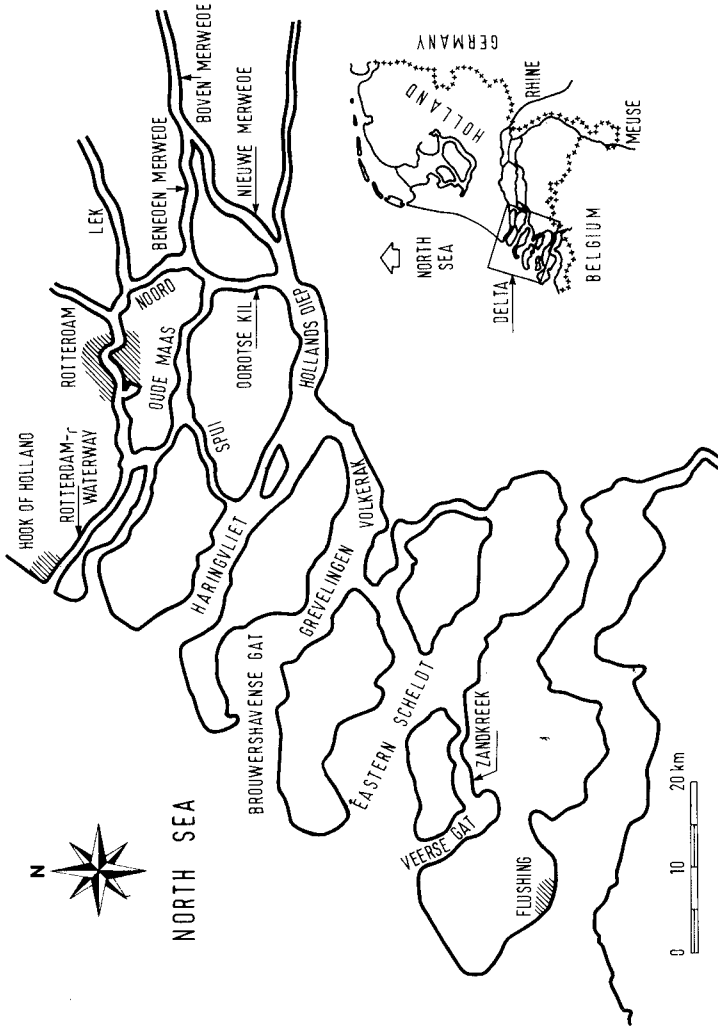


Figure 1. Rhine-Meuse Delta prior to 1953.

of the Eastern Scheldt, Brouwershavense Gat and Haringvliet. To properly manage the Delta and in particular to minimize maintenance dredging and to prevent dike calamities it is important to be able to predict scour and shoaling associated with the various man-made modifications. For this purpose, empirical relations between characteristics of cross-section and flow are derived using observations in the Rhine-Meuse Delta, prior to the Delta project.

2 EQUILIBRIUM FLOW AREAS

The important parameters governing the cross-sectional area at the mouth of the estuaries are the sediment transport capacity of the tidal currents, Q_{tc} , and the littoral drift, Q_l . Assuming that during the major part of the tidal cycle the bottom shear stress is considerably larger than the critical shear stress for sediment motion, the sediment transport capacity of the tidal currents can be expressed as, Leliavsky (1966).

$$Q_{tc} = f(b, F, \rho_s, \rho_w, g, d) \left(\frac{Q}{A}\right)^n \quad (1)$$

in which

Q_{tc}	= sediment transport (m^3/sec)
b	= inlet width
F	= bottom friction
ρ_s	= density of sediment
ρ_w	= density of water
g	= gravity acceleration
d	= grain diameter
Q	= discharge
A	= cross-sectional area

Depending on the investigator, n varies between 3 and 5.

It is postulated that for long term equilibrium conditions

$$\overline{Q}_{tc} :: \overline{Q}_l \quad (2)$$

where the overbar denotes a long term (yearly) average, and thus,

$$\overline{\left(\frac{Q}{A}\right)^n} :: \frac{\overline{Q}_l}{f} \quad (3)$$

For tidal inlets with zero fresh water inflow $\overline{Q} = \text{const.}$ \hat{Q} where \hat{Q} is the maximum discharge during the tidal cycle. Assuming a constant area $A = A_c$, Eq. (3) can be written as

$$\overline{\left(\frac{\hat{Q}}{A}\right)^n} :: \frac{\overline{Q}_l}{f} \quad (4)$$

From observations and restricting attention to inlets in the same geographical area, it follows $\hat{Q}/A_c \approx \text{constant}$, Jarrett (1976), Byrne et al. (1980). Thus, with regard to the long term equilibrium, the magnitude of the littoral drift and the sediment characteristics appear to be of secondary importance. Note that for $n = 3$ the left-hand side of Eq. (4) can be interpreted as the work done by the tidal currents on the inlet bottom per sec.

Similarly to the inlets an attempt is made to correlate the cross-sectional area at the mouth of the estuaries in the Rhine-Meuse Delta with the maximum tidal discharge \hat{Q} . Because in general estuaries have fresh water inflow, the tidal discharge follows from

$$Q(t) = Q_r + \hat{Q} \sin \omega t \quad (5)$$

$Q(t)$ = instantaneous discharge

Q_r = river discharge

$\omega = 2\pi/T$ = angular frequency of the tide

T = tidal period

In this study, the maximum tidal discharge, \hat{Q} , is computed from the measured value of the tidal volume (tidal volume is sum of flood volume and ebb volume) using the equation.

$$TV = \hat{Q} T \left[\frac{Q_r}{\hat{Q}} + \frac{2}{\pi} \sqrt{1 - \left(\frac{Q_r}{\hat{Q}}\right)^2} \right] \quad (6)$$

This equation assumes $Q_r < \hat{Q}$.

For the purpose of this discussion, the cross-section characterizing the estuary mouth is taken at the location where there exists a pronounced change in the rate of change of the cross-sectional area; see Fig. 2. It appears that at this location the characteristic velocity, \bar{v} , defined as the tidal volume divided by the tidal period is a maximum.

For the mouths of the estuaries values of cross-sectional area and maximum tidal discharge are plotted in Fig. 3. To a very good approximation

$$A_c = 1.17 \hat{Q} \quad (7)$$

Here the maximum discharge, \hat{Q} , in Eq. (7) refers to average tide conditions. The corresponding maximum tidal velocity for the estuary mouths is:

$$\hat{u} = 0.85 \text{ m/sec} \quad (8)$$

This value varies slightly for the different estuaries and ranges between 0.82 m/sec and 0.86 m/sec; see van de Kreeke and Haring (1979). For spring tide conditions, the corresponding maximum tidal

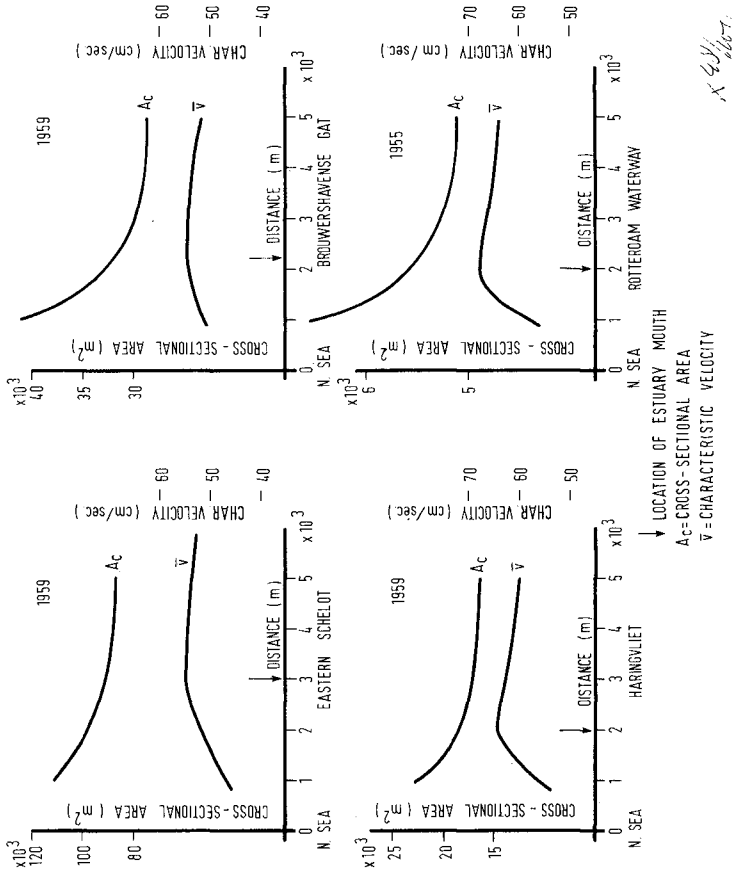


Figure 2. Variation in cross-sectional area and tidal velocity, \bar{v} , along longitudinal axis of estuaries.

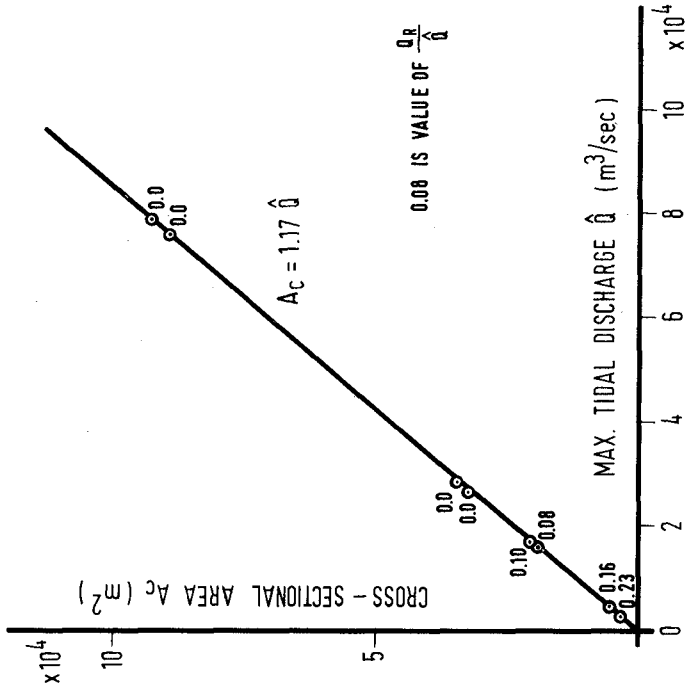


Figure 3. Relation between equilibrium flow area and maximum tidal discharge for estuary mouths.

velocity in the estuary mouths is:

$$\hat{u} = 1 \text{ m/sec} \quad (9)$$

For the values encountered in the Rhine-Meuse Delta, $Q_r/\hat{Q} < 0.25$, the effect of the ratio Q_r/\hat{Q} on the equilibrium flow area appears to be negligible. This is somewhat unexpected as it is generally believed that for constant values of the maximum tidal discharge \hat{Q} , the equilibrium flow area increases with increasing values of the river discharge Q_r . A possible explanation is that the increased cleansing effect resulting from the increased ebb velocities is offset by the inward-directed density currents along the bottom.

It is shown in van de Kreeke and Haring (1979) that Eq. (7) implies that for the Rhine-Meuse Delta the cross-sectional areas at the mouths of the estuaries is proportional to the flood volume rather than the tidal volume.

3 STABILITY CONSIDERATIONS

Because of the time varying nature of the sediment transport capacity of the tidal currents, Q_{TC} , and the littoral drift, Q_d , it is to be expected that cross-sectional areas show variations in time about the long term equilibrium profile. As an example the observed variations in the cross-sectional area of Wachapreague Inlet, Virginia are presented in Fig. 4. The record clearly shows a yearly cycle. Variations are on the order of 10% of the yearly mean value of the cross-sectional area.

If as a result of the short term fluctuations, the cross-sectional area decreases below a certain value, the estuary mouth could conceivably close. This will be explained using Fig. 5 which is taken from Escoffier (1940).

In Fig. 5 the solid curve, further referred to as closure curve is analogous to the well-known relation between inlet velocity and cross-sectional area for bay-inlet systems. In principle, for estuary mouths the closure curve can be obtained by computing the tidal velocity for various values of the cross-sectional area at the mouth. E.g., see Dronkers (1964), chapter XII. The exact shape of the curve depends among other things on how the cross-sectional area is varied i.e., by a change in width or a change in depth. Here it will be assumed that the cross-sectional area, A_c , is gradually decreased by decreasing the water depth. In that case for larger values of A_c , a decrease in cross-sectional area leads to an increase in tidal velocity, \hat{u} . For smaller values of A_c frictional effects become increasingly important and a decrease in cross-sectional area will lead to a decrease in tidal velocity. The horizontal line in Fig. 5 represents Eq. (8), and will be further referred to as the sediment curve.

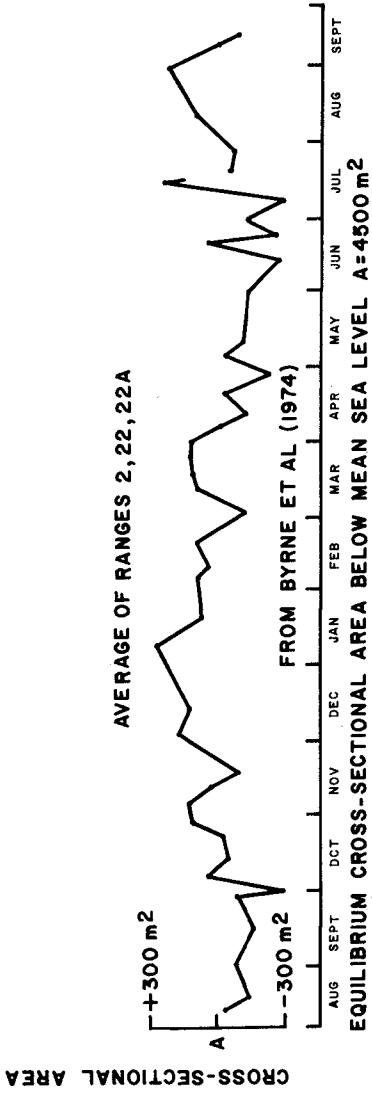


Figure 4. Variations in cross-sectional area for Wachapreague Inlet.

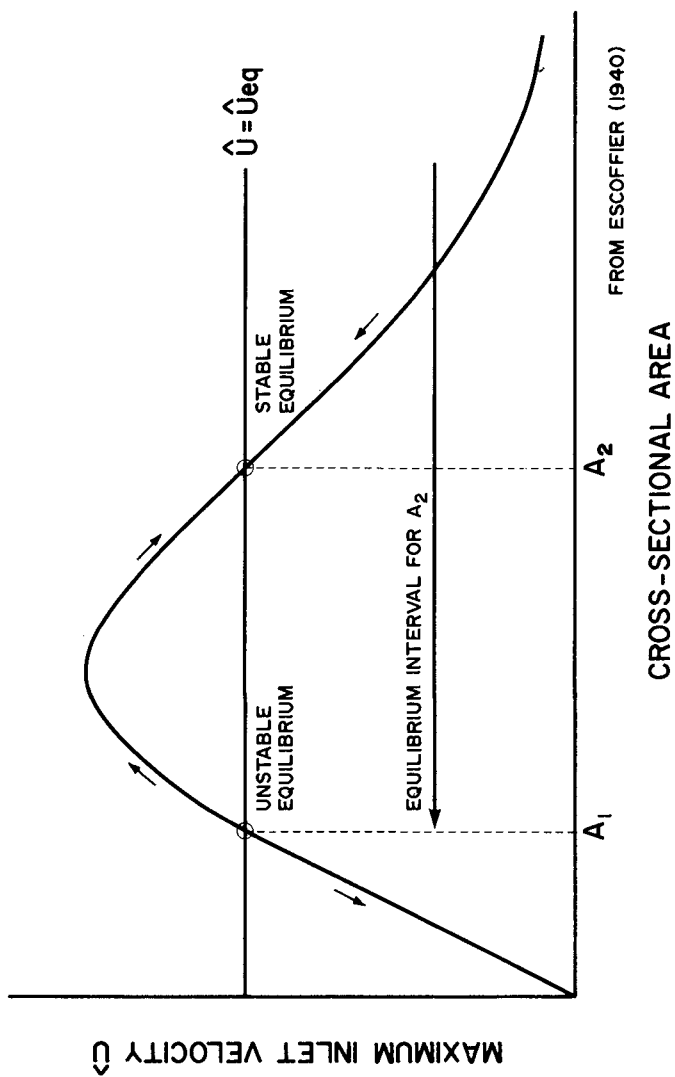


Figure 5. Escoffier diagram.

It follows from Fig. 5 that for values of the cross-sectional area are smaller than A_1 , tidal velocities are too small to maintain the cross-sectional area; the estuary mouth will shoal. For values larger than A_1 the tidal velocity is larger than the velocity required to maintain the cross-sectional area; the estuary mouth will enlarge until the cross-sectional area reaches the value A_2 . Estuary mouths with cross-sections larger than A_2 will shoal until the cross-section reaches the value A_2 . Thus the long-term equilibrium condition for an estuary mouth is represented by the second intersection of the closure and sediment curve.

The foregoing implies that a condition for an estuary mouth to remain open is that the closure curve and sediment curve intersect. As a measure of the degree of stability the ratio $(A_2 - A_1) / A_2$ is introduced. Multiplying by hundred this ratio yields the percentage by which the equilibrium flow area can be reduced before the estuary closes.

As an application of the concepts presented in the previous section variations in the cross-section of the mouth of the Rotterdam Waterway covering the period 1885-1958 are explained. Dredging activities and construction of new harbors during the period 1885-1958, have resulted in a considerable increase of the cross-section at the mouth of the Rotterdam Waterway. A time history of the cross-sectional area and the tidal velocity, u , at the mouth of the estuary, the tidal range at Rotterdam and the various construction activities is presented in Fig. 6. Two equilibrium periods can be identified. The first period between 1897 and 1909 shows a cross-sectional area of 3720 m². During the second period 1944-1958, the equilibrium flow area equals 5600 m².

Closure curves pertaining to the year 1885 and the previously mentioned equilibrium periods together with the sediment curve are indicated in Fig. 7. It is emphasized that the closure curves are not exact but rather show qualitatively the trend of the maximum tidal velocity when changing the cross-sectional area. In 1885 the cross-sectional area of 3000 m², in Fig. 7, was larger than the equilibrium cross-sectional area, a in Fig. 7. During the succeeding period the cross-section would have returned to the equilibrium value were it not for dredging upstream of the mouth. Dredging led to a change in closure curve and caused the cross-sectional area to increase until it reached an equilibrium value of 3720 m² in 1897, in Fig. 7. The cross-sectional area then remained constant until about 1909, when port expansion led to an increase in storage and a change in closure curve. The value of the tidal velocity became larger than the equilibrium value of 0.85 m/sec which led to scour at the mouth of the estuary. However, the process of natural adjustment could not keep pace with the increased storage associated with the construction of harbor basins. Only after 1923 when the pace of harbor construction and dredging reduced did the value of the tidal velocity decrease, in Fig. 7. With the additional help of dredging in the mouth, the cross-sectional area reached a new equilibrium value of 5600 m² in 1944, in Fig. 7. Because relatively little

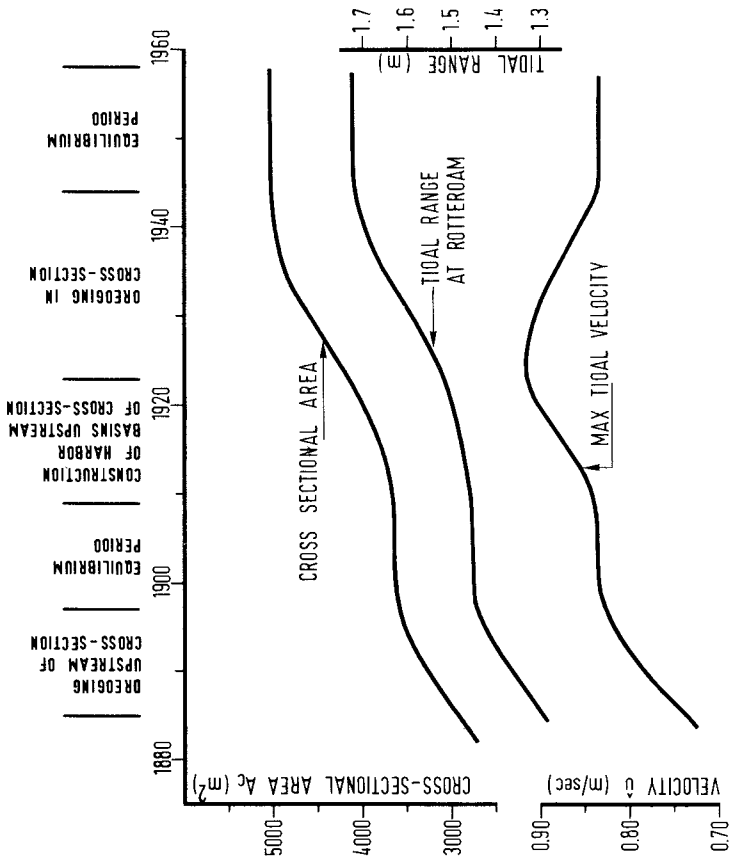


Figure 6. Mouth of Rotterdam Waterway; variations in cross-sectional area, tidal range and maximum tidal velocity during the period 1885-1958.

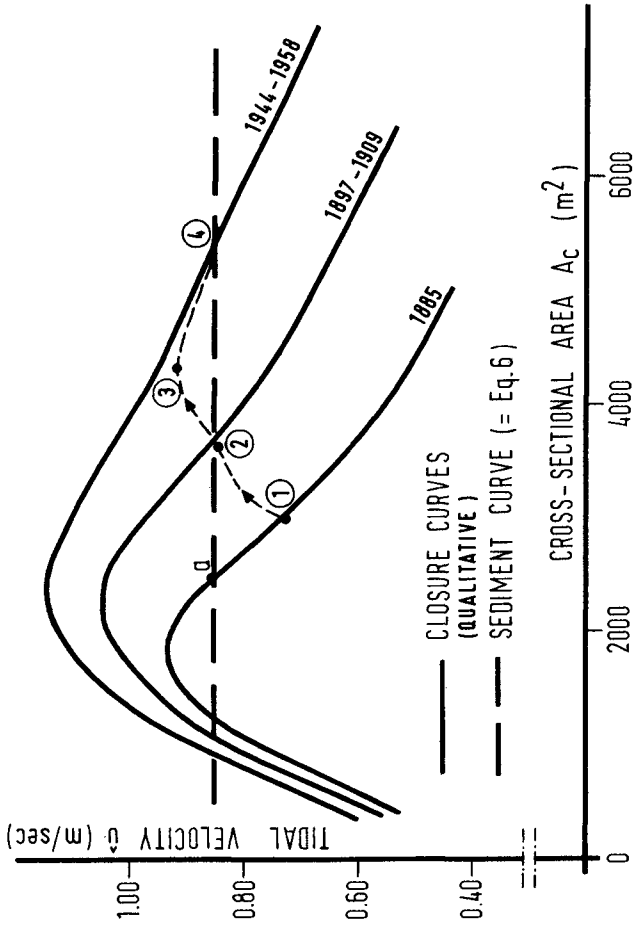


Figure 7. Mouth of Rotterdam Waterway; closure curves and sediment curve.

construction and dredging was carried out during the following period, stable conditions prevailed until 1958. Note that during the period 1885-1958 the stability index for the mouth had considerable increased.

5 CONCLUSIONS

For equilibrium conditions the maximum tidal velocity in the estuary mouths is constant and for average tide conditions equals 0.85 m/sec. For the estuaries with freshwater inflow this implies an approximately constant ratio between flood volume and cross-sectional area. For the estuaries with zero freshwater inflow the implication is a constant ratio between tidal prism and cross-sectional area.

Variations in the cross-sectional area at the mouth of the Rotterdam Waterway during the period 1885-1958 are explained using closure curves and a sediment curve (Escoffier diagram).

REFERENCES

- BYRNE, R.J., J.T. DeALTERIS and P.A. BULLOCK, (1974). "Channel Stability in Tidal Inlets: A Case Study," Proceedings 14th Coastal Engineering Conference, Copenhagen, Vol. II.
- BYRNE, R.J., R.A. GAMMISCH and G.R. THOMAS, (1980). "Tidal Prism-Inlet Area Relations for Small Tidal Inlets," Proceedings 17th Coastal Engineering Conference, Sydney.
- DRONKERS, J.J., (1964). "Tidal Computations in Rivers and Coastal Waters," North Holland Publishing Co., Amsterdam.
- ESCOFFIER, F.F., (1940). "The Stability of Tidal Inlets," Shore and Beach, Vol. 8. No. 4.
- JARRETT, J.T., (1976). "Tidal Prism-Inlet Area Relationships," Department of the Army, Corps of Engineers, U.S. Army Coastal Engineering Research Center and U.S. Army Engineers Waterways Experiment Station, CITI Report No. 3.
- LELIAVSKY, S.L., (1966). "An Introduction to Fluvial Hydraulics," Dover Publications, Inc., New York.
- TERWINDT, J.H.J., (1973). "Sand Movement in the In - and Offshore Tidal Area of the S.W. Part of the Netherlands," Geol. Mynbouw, 52(2): 69-77.
- VAN DE KREEKE, J. and J. HARING, (1979). "Equilibrium Flow Areas in the Rhine-Meuse Delta," Coastal Engineering, 3, 97-111.